Probing deeper: Determining the 3D γ-γ'- microstructure in a Ni-base superalloy by FIB-SEM tomography

Background

- Excellent mechanical properties of Ni-base superalloys due to γ-γ'-microstructure
- Investigation of 3-dimensional microstructure to understand and improve these superalloys
- Scanning Electron Microscopy (SEM) to image the microstructure: suitable contrast, resolution and field of view
- Combine with serial ablation by Focused Ion Beam (FIB): image stack for 3D reconstruction
- Improve contrast by chemical etching not possible during FIB experiment → use of adequate detector

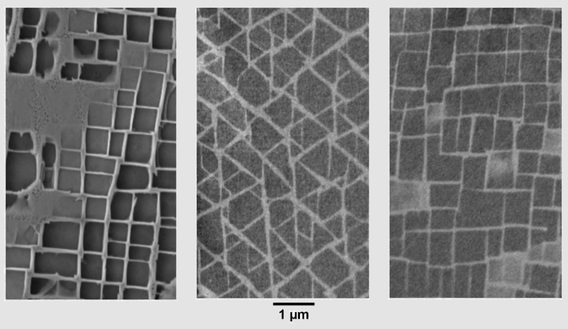

Fig.1: SEM micrograph of CMSX-4 samples: chemically etched in a), untreated with a circular backscatter detector (CBS) in b) and the same sample aligned and rotation corrected in c).

Experimental

- Sample: ERBO 1C (cast CMSX-4 alloy) [1]
- Use of CBS impeded in conventional FIB-SEM setup (compare fig.2 (b))
- Modified setup for use of retractable detector (fig.2 (c))
- Special considerations about the image alignment because of the new ablated volume geometry (see fig.2 (c) and fig.3)
- Software used for correction, segmentation, and analysis: AVIZO, ilastik, imageJ

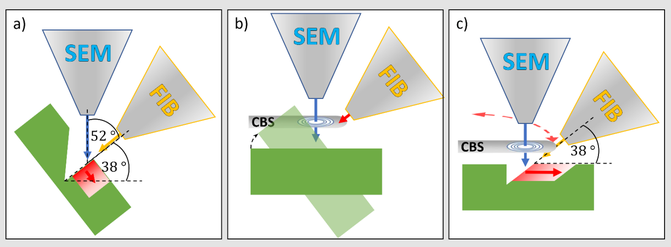

Fig.2: Conventional setup for FIB-SEM tomography (a). Insertion of a CBS interferes with tilted sample and FIB (b). Modified setup with retractable CBS (c) allows for acquiring a high-contrast image series of a sample volume with tilted cuboid geometry.

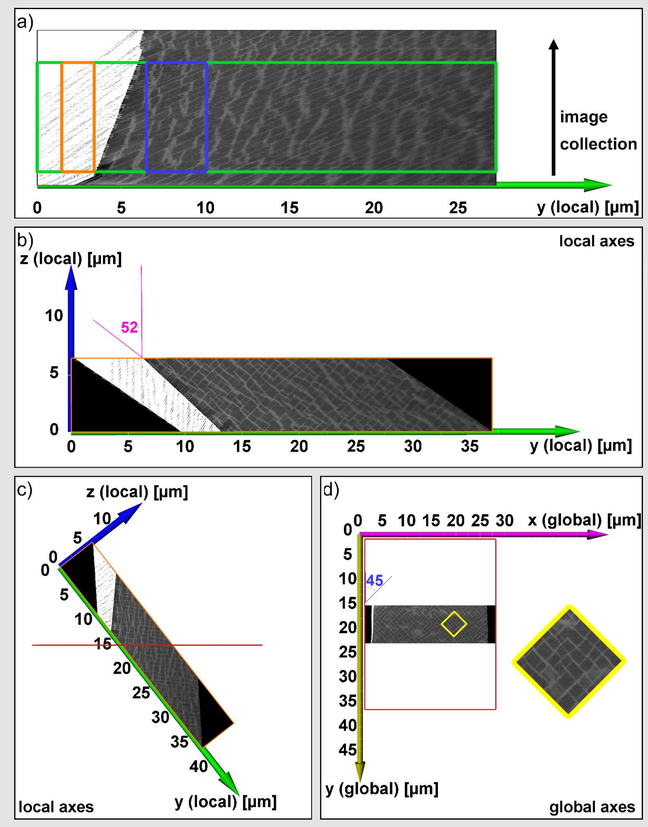

Fig.3: Planar view of the uncorrected sample with two regions of interests for alignment (orange and blue frames) in a). Aligned sample in b). c) shows the rotation corrected sample as indicated in b), the red line indicates the image plane shown in d).

Sample Extraction, Visualization, and Segmentation

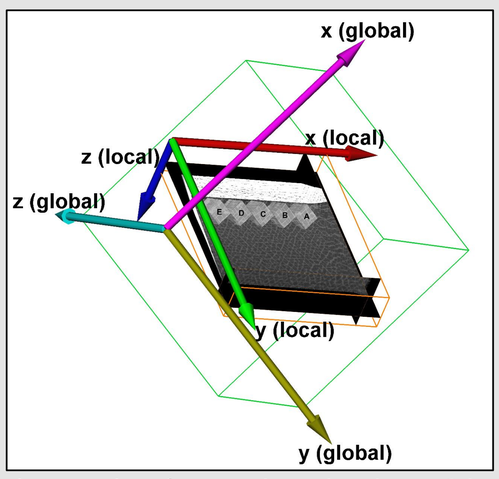

Fig.4: Location of extracted sample volumes. Color code for local and global axes chosen as in fig.3.

- 5 sample volumes extracted for further analysis, each with equal sizes and voxel dimensions of x = 19.2165 nm, y = 24.386 nm and z = 10 nm
- Probability maps, binarization, object separation for segmentation according to γ and γ'

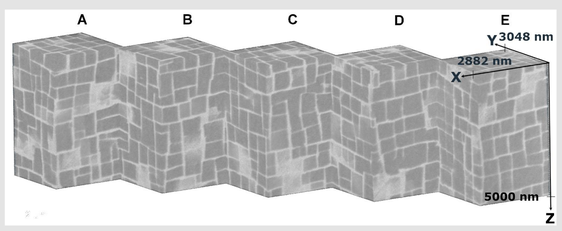

Fig.5: Sample volumes before segmentation.

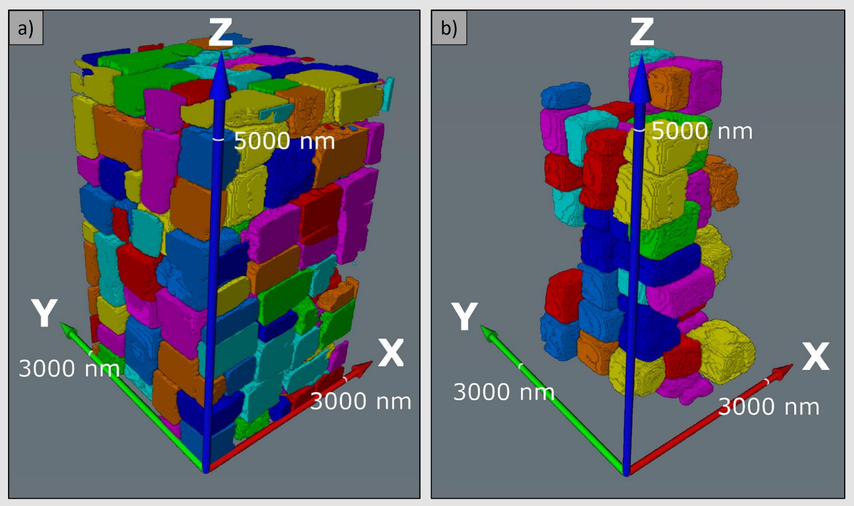

Fig.6: Segmented and volume rendered depiction of the γ' particles in sample volume B (a). The same volume shown without particles touching the volume border (b).

Analyses and Discussion

- 3D analysis → particle shape factor $\psi = \frac{S_{V,particle}}{S_{V,equ\ cube}}$
- Both 2D & 3D analysis → phase fractions
- 2D analyses (line intersect method) → Channel and particle widths

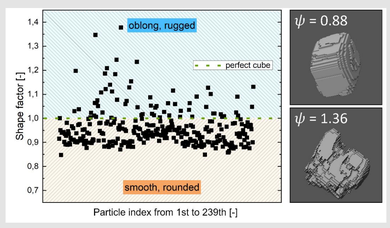

Fig.7: Particle shapes. The green line indicates the shape factor of a cubic particle. Factors $\psi < 0$ indicate rounded particles, factors $\psi > 0$ indicate rugged or elongated particles.

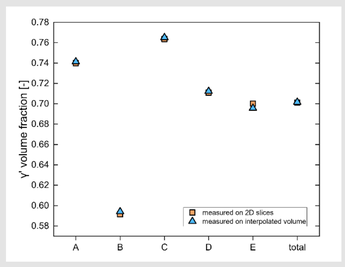

Fig.8: γ' phase volume fraction determined on volume (voxel representation, 3D) and on slices (pixel representation, 2D).

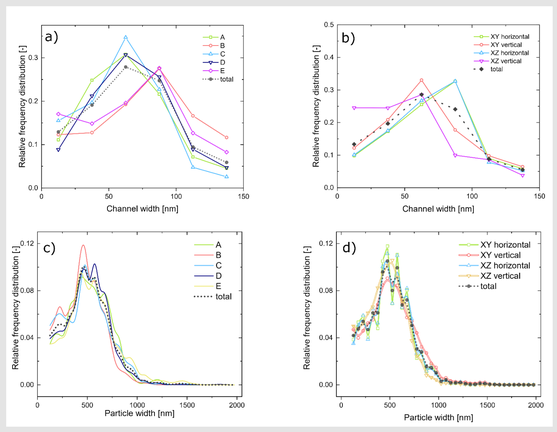

Fig.9: γ channel width discriminated by sample volume (a) and by direction of the line intersects (b), group size 25 nm. γ' particle width discriminated by sample volume (c) and by direction of line intersects (d), group size 50 nm.

Tab.I: Mean γ channel widths and γ' particle widths with standard deviation discriminated by sample volumes and combined totals. The deviation from the respective mean values of 69 nm (γ) and 461 nm (γ') in [2] is given.

Phase	γ						γ'					
Sample volume	A	B	C	D	E	Total	A	B	C	D	E	Total
# data points	68011	53496	80114	70631	57827	319891	46246	71965	84386	80196	71809	354602
$x_{mean} \pm$ StdDev [nm]	65.3±31.2	79.6±37.9	61.5±29.6	69.2±31.4	72.1±36.8	68.7±33.6	514±213	461±192	496±224	506±206	547±249	504±220
Dev. x_{mean} from [2] [%]	5.4	15.4	8.9	0.3	4.5	1.0	11.5	0.0	7.6	9.8	18.7	9.3

- γ size, γ' size in accordance with literature [2]
- γ' phase fraction in accordance with literature (0.23 % and 0.97 % deviation from [2] and [3], respectively)

- Phase fraction congruency → no artifacts from 2D to 3D interpolation

- Artifacts and sources of errors:
  - limited and coarse discrete distribution of possible length values (10 nm - 24.386 nm steps due to voxel dimensions)
  - ambiguous textural features of channel-particle edges → 'grainy' binarization = rugged surfaces
  - overly aggressive separation algorithm, virtual erosion
  - undersegmentation

Conclusions

- Good accordance of evaluated descriptors from 2D and 3D representations with literature
- Coarse distribution of possible measurement values due to resolution of examined volumes
- Improvement of sample size by aligning the {100} sample plane with ablated surface → maintain original resolution & no interpolation necessary
- Approach can be used to e.g. calibrate stereographic reconstructions or determine parameters for 3D microstructure simulations

References: [1] https://www.sfb-transregio103.de
[2] B. Ruttert, D. Bürger, L. M. Roncery, A. B. Parsa, P. Wollgramm, G. Eggeler and W. Theisen, Mater. Des., 2017, vol. 134, pp. 418-425.
[3] M. Ramsperger, R. F. Singer and C. Körner, Metall. Mater. Trans., A 2016, vol. 47, pp. 1469-1480.

A. Dennstedt*, F. Kreps, T. Schwope, M. Bartsch
German Aerospace Center, Institute of Materials Research, Linder Höhe, 51147 Cologne, Germany
*Corresponding author: anne.dennstedt@dlr.de

DLR Deutsches Zentrum für Luft- und Raumfahrt

SFB/Transregio 103 SUPERALLOY SINGLE CRYSTALS